DOI 10.5162/Ultrasonic2025/C2-a2

3D imaging with Scanning Acoustic Microscopy – A comparison of the focusing capabilities of array transducers and Synthetic Aperture with highly focused transducers

Mario Wolf[1], *Emanuel Leipner*[1], *Stefan König*[3], *Peter Hoffrogge*[3], *Peter Czurratis*[3], *and Christian Kupsch*[1,2]
[1] *TU Bergakademie Freiberg, Measurement, Sensor and Embedded Systems Lab (MSE Lab), Freiberg, Saxony, Germany*
[2] *TU Bergakademie Freiberg, Center for Efficient High Temperature Processes and Materials Conversion (SN0390002), Freiberg, Saxony, Germany*
[3] *PVA TePla Analytical Systems GmbH, Westhausen, Baden-Württemberg, Germany*
mario.wolf@mse.tu-freiberg.de

Abstract: This paper investigates the potential of Scanning Acoustic Microscopy (SAM) for 3D inspection of modern electronic devices using a single scan. Two complementary approaches to focus on different internal interfaces are examined: the Synthetic Aperture Focusing Technique (SAFT) utilizing a conventional SAM transducer and beaforming applied on an annular array transducer. A detailed comparison of both methods is presented. The image evaluation reveals that the SAFT approach delivers superior performance in terms of resolution and clarity.

Keywords: Scanning Acoustic Microscopy (SAM), 3D inspection of microelectronic devices, Synthetic Aperture Focusing Technique (SAFT), Annular Arrays, Signal processing

Introduction

Scanning Acoustic Microscopy (SAM) is a well-established tool in failure analysis and quality assurance. Traditionally, it has been standard practice to inspect commonly bonded interfaces to detect delaminations or misalignments. Earlier technologies, such as flip-chip packaging, typically required only a two-dimensional evaluation of a single interface. In contrast, modern manufacturing approaches—exemplified by System-in-Package (SiP) designs — necessitate comprehensive three-dimensional inspection. High-Bandwidth Memory (HBM), for instance, consists of a stack of at least eight silicon dies, all of which must be examined. In power electronics, the complexity increases further, with structures such as bond wires routed non-parallel to the surface, posing additional challenges for inspection.

To meet the required detection limits, SAM uses transducers operating within the range of $20\,\mathrm{MHz}$ to $2000\,\mathrm{MHz}$, depending on the specific requirements of the application in consideration. To achieve high resolution, these transducers are characterised by a high degree of focusing, resulting in minimal lateral extension of the focus spot and a correspondingly minimal depth of field. Therefore, it can be concluded that a single scan is capable of producing a sharp image of a single interface with precise focus at the point of interest. However, images of interfaces before or beyond the focus are significantly blurred. For sharp images of all interface several scans need to be performed. Consequently, conventional SAM imaging is forced to compromise between inspection time and the probability of detecting small defects. To overcome this tradeoff, SAFT and annular array focusing can be aplied, allowing focusing in different depths by postprocessing measurement data from a single lateral scan.

The efficacy of the Synthetic Aperture Focusing Technique (SAFT) in enhancing the performance of the inspection process has been demonstrated through its successful implementation [1]. SAFT works by superposing pre-processed signals from multiple measurement positions for each imaging point. This creates a virtual transducer with a synthetic aperture that focuses at a specific depth. SAFT has been demonstrated using laboratory [2] and industrial samples, including an HBM stack [3]. SAFT can be applied with standard single-element SAM transducers.

In other areas of ultrasonic applications, there are many different transducer designs. Phased array probes are a common part of medical ultrasound and low frequency NDT applications. A three-dimensional image can be created by scanning only one line, while focusing in the other two dimensions is achieved through various methods [Huang, 2017]. However, phased arrays consist of 64, 128 or more elements and require advanced technology to manufacture, as well as complex electronics to generate pulses and

DOI 10.5162/Ultrasonic2025/C2-a2

detect signals. Therefore, phased arrays operating at frequencies of $100\,\mathrm{MHz}$ or higher continue to be the focus of theoretical simulation studies.

In contrast, annular arrays consist of several concentric, ring-shaped elements. Typically, only six to ten elements are required to generate a focal spot approximately one wavelength in size, which can be shifted along the acoustic axis. Annular arrays are fabricated using either PVDF [4] or CMUT technology [5] with center frequencies around $50\,\mathrm{MHz}$ are available. As demonstrated in [6], it is well established that thin films of ZnO can be structured accordingly. Therefore, ZnO is a suitable material for the fabrication of annular array structures working above $100\,\mathrm{MHz}$.

The objective of this investigation is to compare the achievable resolutions for different measurement depths from a single lateral scan for three approaches: direct focusing with a single transducer, SAFT reconstruction, and focusing using an annular array. To this end, a customized annular array was designed, taking into account current manufacturing constraints. Sound field simulations were carried out to predict the performance of the proposed design. The evaluation focuses on the detection of delaminations at silicon–copper interfaces for various silicon layer thicknesses.

Methods

Sound field simulation

Sound field calculations are performed using harmonic Green's functions in combination with point source synthesis and a separation approach [7]. The surface of the piezoelectric element is used as the source area, and the stress distribution on the lens surface is computed accordingly. This stress distribution serves as a novel source for calculating the resulting stress distribution on the silicon surface. This approach allows the calculation of the sound field distribution within the silicon sample or on its backside. To obtain time-domain signals, stress components must be calculated for a set of frequencies. Harmonic synthesis is then carried out via the inverse Fourier transform.

SAFT with conventional SAM Transducers

Conventional SAM measurements are performed by scanning an area in the lateral xy-plane. At each scan position, an ultrasonic wave is excited, and the reflected signal is recorded. In the case of C-scan imaging, the maximum amplitude at a defined depth is evaluated and color-coded for each individual pixel. The complete signal is recorded at every position, resulting in a 3D dataset for subsequent processing. For SAFT reconstruction, the phase shift migration (PSM) technique is employed [8]. The 3D dataset is transformed into the frequency domain, multiplied by a phase term, and then transformed back into the time domain. This phase term depends on the sound velocity and the distance between the source and the reconstruction depth.To apply SAFT to SAM data, the transducer's focal point is assumed to act as a virtual point source for the purpose of reconstruction. According to the Near-Field SAFT approach [3], reconstruction can be performed at arbitrary depths—even if the focal point is located beyond the sample.

Beamforming with annular arrays

In most applications involving array transducers, time shifts for beamforming are determined using simple geometric models. Each array element is represented by a discrete attachment point, and the distance from each point to the designated focus position is calculated. Time-of-flight differences are then derived under the assumption of a constant speed of sound in a homogeneous propagation medium.

These time-of-flight differences are used to delay the individual signals prior to their superposition. In the case of the array used in this study, however, the wave propagates from the element through a lens body, is then focused by a spherically shaped calotte, and undergoes refraction as it passes from water into silicon. Due to the complex geometry and the significant refraction at the interface, geometric approximations for the wave propagation prove insufficient in this case. Instead, we make use of simulation data, in which the phase information for each frequency and array element has been precomputed. Beamforming is then achieved by applying phase shifts to the harmonic sound fields, such that all components constructively interfere at the designated focus position.

Generation of simulation data

The 8mm-VHF$+$ transducer operating at a frequency of $180\,\mathrm{MHz}$ (PVA TePla, Westhausen, Germany) was selected for use as a single-element transducer. A water path of $0.8\,\mathrm{mm}$ was chosen. The amplitude distribution is color-coded in decibels (dB) and normalized to its individual maximum. The sound fields in silicon are calculated for both, the single-element transducer, Fig. 1, and for the six array elements, Fig. 2. The geometry of the array elements is summarized in Tab. 1. The elements are located at the rear side of a lens body, which has a total length of $12\,\mathrm{mm}$ and a spherically shaped calotte with a radius of curvature of $20\,\mathrm{mm}$.

The reflected signal was calculated assuming silicon layers of different thicknesses z, followed by copper, Fig. 3 left. For this purpose, the stress distribution at the corresponding depth was computed. The reflec-

DOI 10.5162/Ultrasonic2025/C2-a2

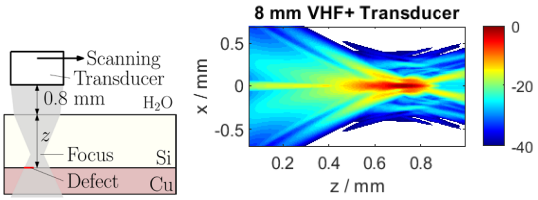

Fig. 1: left: sketch of the simulated setup and right: Sound field of the 8mm-VHF+ Transducer

Tab. 1: Geometry of the annular array with the inner radii r_i and the outer radii r_a of each element

Element	1	2	3	4	5	6
r_i / mm	0	0.72	1.03	1.27	1.48	1.67
r_a / mm	0.68	0.99	1.23	1.44	1.63	1.80

tion coefficient for the defect-free silicon-to-copper interface is 0.39. For a smaller area of $50\,\mu\mathrm{m}$ x $50\,\mu\mathrm{m}$, the reflection coefficient was set to -1, modeling a delamination. The scan data were generated by a 2D convolution of the local reflection coefficients with the signals at the interface. For both transducers, layer thickness z of $0.4\,\mathrm{mm}$, $0.6\,\mathrm{mm}$ and $0.9\,\mathrm{mm}$ were selected. Furthermore, echoes for a layer whose backside is located within the focus of the 8mm-VHF+ transducer at $0.736\,\mathrm{mm}$ were calculated. This reference is used to evaluate image quality. Fig. 3 right illustrates the resulting scan data for the focused scan (top left) and the defocused scans. Additionally, signals obtained from scanning were calculated for all six array elements and all three layer thicknesses.

Results and discussion

Three examples of SAFT reconstructions are shown at the top of Fig. 4. The delamination at $z = 0.6\,\mathrm{mm}$ is reconstructed with greater clarity than at $z = 0.4\,\mathrm{mm}$, which can be attributed to the smaller distance between the defect and the focal point. This observation is consistent with the expected increase in near-field effects at shallower depths (see Fig. 1). In both cases, the structures are surrounded by zones of reduced amplitude. At $z = 0.9\,\mathrm{mm}$, a loss of contrast and an apparent enlargement of the defect are observed. The reduced reconstruction quality results from a significant portion of the reflected wave not returning to the transducer, leading to a loss of signal energy and information. The images obtained using annular array focusing, Fig. 4 bottom, exhibit low contrast and an overestimated defect size. As shown in Fig. 5, the amplitude distribution along a single scan line allows a direct comparison between annular array focusing

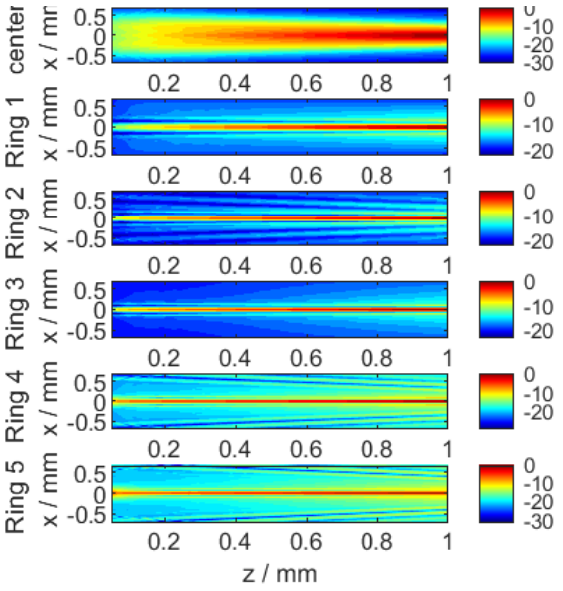

Fig. 2: Sound field of the 6 array elements.

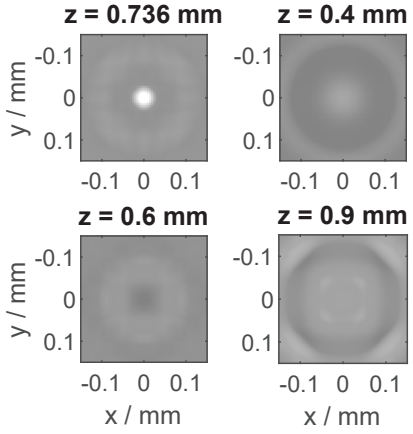

Fig. 3: Scan with 8mm-VHF+ Transducer in focus and for 3 depths out of focus.

(left) and SAFT reconstruction with the 8mm-VHF+ transducer (right). Compared to the amplitude profiles from the directly focused scan (black lines), it becomes clear that only SAFT reconstructions in the near field yield sufficiently accurate results. Even in these cases, a moderate reduction in contrast is observed.It must be noted that the annular array does not meet performance expectations. Despite the high number of degrees of freedom in its design, the array was configured according to established guidelines [4]. All elements have equal surface area to ensure consistent near-field length, and both the lens body length and radius of curvature were selected such that no near-field structures occur within the depth range relevant for the measurements (see Fig. 2). These findings stand in contrast to previous results and applications

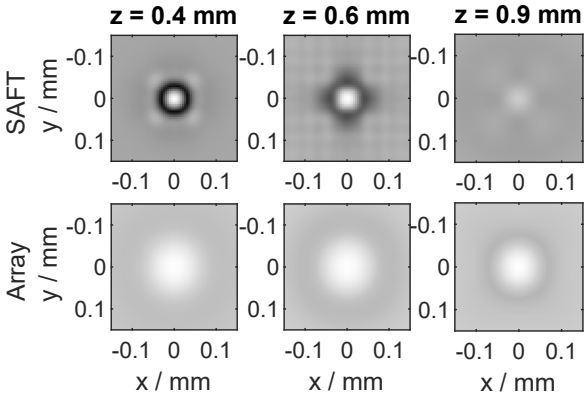

Fig. 4: Calculated images for three different depths; top: SAFT reconstruction with the 8mm-VHF+ Transducer and bottom: focused images obtained with the annular array.

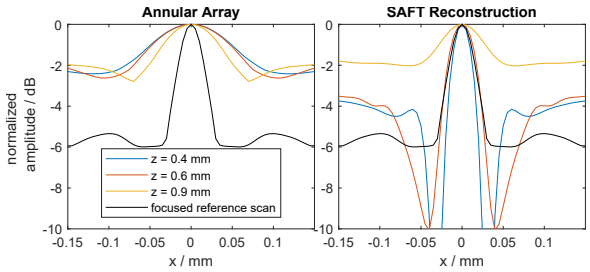

Fig. 5: Comparison of the amplitudes along a line scan; left: focusing with the annular array and right: the SAFT reconstruction.

of annular arrays in fluid environments.

Conclusion

The comparison of reconstruction results demonstrates a clear improvement in performance when applying the Near-Field SAFT algorithm. In contrast, both the far-field SAFT reconstruction (see Fig. 5, yellow line) and the beamforming results obtained with the annular array show reduced contrast and an overestimation of structure size, indicating a loss of resolution. The findings of this study suggest that annular arrays, in their current form, are not well suited for use in SAM. To enable their practical application, the focusing resolution must be significantly improved. This requires a broad parameter space and, consequently, the development of revised design rules. Existing guidelines, derived for configurations with homogeneous sound velocity or simple geometries, appear to be insufficient for more complex cases involving refractive interfaces. It should also be noted that all array designs remain subject to manufacturing constraints. The present design was selected based on current fabrication capabilities, and experimental validation of the simulation results is still pending. Nevertheless, this study provides an initial theoretical assessment of the Near-Field SAFT algorithm's performance. By systematically varying the assumed layer thicknesses, key performance characteristics can be derived, and the applicable limits of the algorithm can be defined.

Acknowledgments

The authors would like to thank the DFG for financial support in the Project 427525397.

References

[1] M. Wolf et al. "Inspection of multilayered electronic devices via scanning acoustic microscopy using synthetic aperture focusing technique". In: *2022 IEEE International Ultrasonics Symposium (IUS)*. IEEE. 2022, pp. 1–4.

[2] C. Kupsch and M. Wolf. "Nonlinear beamforming for Scanning Acoustic Microscopy Imaging through scattering surfaces". In: *2023 IEEE International Ultrasonics Symposium (IUS)*. IEEE. 2023, pp. 1–4.

[3] M. Wolf et al. "Near-Field Synthetic Aperture Focusing Technique to enhance the inspection capability of multi-layer HBM stacks in Scanning Acoustic Microscopy". In: *International Symposium for Testing and Failure Analysis*. Vol. 84741. ASM International. 2023, pp. 448–451.

[4] J. A. Brown, C. E. Demore, and G. R. Lockwood. "Design and fabrication of annular arrays for high-frequency ultrasound". In: *IEEE transactions on ultrasonics, ferroelectrics, and frequency control* 51.8 (2004), pp. 1010–1017.

[5] J. Zahorian and F. L. Degertekin. "Modeling and characterization of thin film coatings for high frequency CMUT annular arrays". In: *2011 IEEE International Ultrasonics Symposium*. IEEE. 2011, pp. 596–599.

[6] A. Kumar et al. "Design, fabrication and reliability study of piezoelectric ZnO based structure for development of MEMS acoustic sensor". In: *Microsystem Technologies* 25.12 (2019), pp. 4517–4528.

[7] E. Kühnicke. "Three-dimensional waves in layered media with nonparallel and curved interfaces: A theoretical approach". In: *The Journal of the Acoustical Society of America* 100.2 (1996), pp. 709–716.

[8] T. Olofsson. "Phase shift migration for imaging layered objects and objects immersed in water". In: *IEEE transactions on ultrasonics, ferroelectrics, and frequency control* 57.11 (2010), pp. 2522–2530.